

# Percolation exponents and thresholds obtained from the nearly ideal continuum percolation system graphite-boron nitride

Junjie Wu and D. S. McLachlan

*Department of Physics and Condensed Matter Physics Research Unit, University of the Witwatersrand, P.O. WITS 2050, Johannesburg, South Africa*

(Received 20 May 1996; revised manuscript received 28 October 1996)

Compressed disks made from graphite and, its mechanical but not electrical isomorph, boron nitride as well as graphite-boron nitride powders, undergoing compression, are nearly ideal continuum percolation systems, as the ratio of their conductivities is nearly  $10^{-18}$  and the scatter of the experimental points near the critical volume fraction  $\phi_c$  is very small. The following measurements, with the characteristic exponent(s) in brackets, are made on some or all of the samples in (axial) and at right angles (radial) to the direction of compression, as a function of the volume fraction of graphite ( $\phi$ ); dc conductivity ( $s$  and  $t$ ), dielectric constant ( $s$ ), magnetoresistivity ( $t_{\perp}$ ), and noise power ( $K$ ). The noise power is also measured as function of resistance ( $w$ ) and volume ( $b'$ ). The  $\phi_c$ 's obtained for all measurements are consistent and explicable. The results for the exponents are less well understood but, where possible, these results are compared with theoretical predictions and previous experiments. The reasons for the nonuniversality of  $t$  are clarified. [S0163-1829(97)00327-5]

## I. INTRODUCTION

The properties of conductor-insulator (or metal-insulator) composites have been extensively studied by both experimental and theoretical physicists for many years. At first mixture rules and later effective media theories were used to analyze the data, but since the 1970s the main theoretical models have involved percolation theory and the concept of scaling. This is due to the realization that the percolation threshold in metal-insulator systems (lattice models, model systems, and continuum composites) is a critical point, analogous to the critical points of phase transitions in thermodynamic systems. Some of the major review articles in this field are by Kirkpatrick,<sup>1</sup> Landauer,<sup>2</sup> Bergman and Stroud,<sup>3</sup> and Nan.<sup>4</sup> In addition there is an extensive set of review articles on percolation processes in the book, edited by Deutscher, Zallen, and Adler<sup>5</sup> and also the revised textbook on percolation by Stauffer and Aharony.<sup>6</sup>

Most experimental work has been focused on the simple dc resistivity properties, less on the ac dielectric or conductivity properties, the Hall effect and flicker noise, and very little on the magnetoresistivity and thermopower. In most experimental papers only one or two of these properties is measured on the same system, which makes it difficult to compare and correlate the different exponents that appear in the various scaling laws, which have the form  $Q \propto |\phi - \phi_c|^x$ . Here  $Q$  is the physical (electrical) property measured,  $x$  the (in some cases universal) exponent,  $\phi$  the volume fraction of the conducting component, and  $\phi_c$  the critical volume fraction or percolation threshold.  $\phi_c$  is the volume fraction where the conducting component first forms an infinite or spanning cluster in the sample or a continuous dc conduction path across an infinite (in practice very large) sample. In this paper we report on measurements of a large number of exponents, together with the  $\phi_c$  value, in two reliable continuum percolation systems and then try to relate them to the theoretically predicted values and those mea-

sured in similar systems. The measurements made (with the corresponding exponent in brackets) were the dc conductivity ( $s$  for  $\phi < \phi_c$  and  $t$  for  $\phi > \phi_c$ ), the real part of the ac dielectric constant ( $s$ , measurable only for  $\phi < \phi_c$ ), the ac conductivity ( $t$  for  $\phi > \phi_c$ ), the ratio of the anisotropic (axial and radial) dc conductivities ( $\lambda$ ), the flicker or  $1/f$  noise ( $w$  and  $K$ ), and the transverse magnetoresistivity ( $t_{\perp}$ ). The dispersion measurements  $\epsilon(\omega)$  (exponent  $u$ , which is related to  $s$  and  $t$ ) and thermopower measurements will be discussed in further publications.

Up until nearly ten years ago it was widely believed that all the exponents, whether measured in a lattice model (computer simulation), a model system or a continuum composite, were universal, in that they depended on the geometrical dimension only—3D in these experiments. Since then it has been realized that there are a number of continuum systems in which unequivocal nonuniversal exponents have been observed or predicted.<sup>4</sup> Many of the exponents presented in this paper are nonuniversal and will be discussed using the currently accepted models for nonuniversal exponents (see theory section).

In Sec. II the equations used are presented and discussed and the experimental procedures are described in Sec. III. The results are presented in Sec. IV and discussed in Sec. V. Our conclusions, made from the discussion, are in Sec. VI.

## II. THEORY

### A. The percolation equations and exponents

When the ratio of the conductivities of the two components of binary disordered conductor-insulator media is not very small ( $\sigma_i/\sigma_c \leq 1$ ), the conductivity of continuum media can sometimes be described by an effective media theory.<sup>2-4,7</sup> However, when this ratio is very small ( $\sigma_i/\sigma_c \ll 1$ ), conductor-insulator systems, especially near  $\phi_c$ , are

best described by percolation theory, which is also a scaling theory for phase transitions.<sup>3,4,6,8,9</sup> A number books<sup>5,6,10</sup> and review articles<sup>1-4</sup> cover percolation theory and compare the results from both lattice and continuum systems with theory. The ‘‘binary’’ system considered in this paper has a conductivity  $\sigma_m(\phi)$  and a complex dielectric constant  $\epsilon_{mr}(\phi) + i\epsilon_{mi}(\phi)[\epsilon_{mi}(\phi) = \sigma_m(\phi)/\omega\epsilon_0]$ , which is made up of a conducting component [ $\sigma_c$  and  $\epsilon_c = \epsilon_{cr} + i\epsilon_{ci}$  (in which  $\epsilon_{cr}$  is usually ignored or put equal to zero and  $\epsilon_{ci} = \sigma_c/\omega\epsilon_0$ )] with a volume fraction  $\phi$ , an insulating component [ $\sigma_i$  and  $\epsilon_i = \epsilon_{ir} + i\epsilon_{ii}$  (in which  $\epsilon_{ii}$  is usually taken to be zero)] and a critical volume fraction or percolation threshold  $\phi_c$ .  $\phi_c$  can only be unequivocally directly measured as the first detectable dc conductivity, in an infinitely (very) large sample when  $\sigma_i/\sigma_c = 0$  because  $\sigma_i = 0$ , or where the dc conductivity becomes  $\infty$  and again  $\sigma_i/\sigma_c = 0$ . In all other cases  $\phi_c$  for continuum systems must be obtained by fitting the data to a theoretical expression(s).

The expressions for  $\sigma_m(0, \phi)[\omega = 0]$ ,  $\epsilon_{mr}(\omega, \phi)$ , and  $\sigma_{mr}^*(\omega, \phi) = \omega\epsilon_0\epsilon_{mr}$  with  $|\phi - \phi_c| = \Delta\phi$ , given to lowest order,<sup>3,4,8,9</sup>

$$\sigma_m = \sigma_c \Delta\phi^t, \quad \epsilon_{mr} = \epsilon_{ir} \Delta\phi^{-s}, \quad \sigma_{mr}^* = \sigma_c \Delta\phi^t \quad [\phi > \phi_c], \quad (1a)$$

$$\sigma_m = \sigma_i \Delta\phi^{-s}, \quad \epsilon_{mr} = \epsilon_{ir} \Delta\phi^{-s},$$

$$\sigma_{mr}^* = (\omega^2 \epsilon_0^2 \epsilon_{ir}^2 / \sigma_c) \Delta\phi^{-t-2s} \quad [\phi < \phi_c], \quad (1b)$$

$$\sigma_m = \sigma_i^u \sigma_c^{1-u}, \quad \epsilon_{mr} = \epsilon_{ir}^u (\sigma_c / \epsilon_0 \omega)^{1-u},$$

$$\sigma_{mr}^* = (\omega \epsilon_0 \epsilon_{ir})^u \sigma_c^{1-u} \quad [\phi \approx \phi_c], \quad (1c)$$

where  $u = t/(s+t)$ . Equations (1c) apply in the region  $|\phi - \phi_c| = \delta$ , given<sup>3,4,8,11</sup> by  $\delta_{dc} = (\sigma_i/\sigma_c)^{1/(t+s)}$  or for ac measurements, with  $\sigma_i \ll \omega\epsilon_0\epsilon_{ir} \ll \sigma_c$  and assuming  $\epsilon_{ii}$ , due to polar losses, is zero or negligible, by  $\delta_{ac} = (\omega\epsilon_0\epsilon_{ir}/\sigma_c)^{1/(t+s)}$ . As  $\sigma_i/\sigma_c$  in this paper is  $10^{-18}$  and  $\omega$  small, the region covered by Eq. (1c) is experimentally inaccessible and will not be further discussed.

If the data covers a large range of  $\phi$  and especially where  $\phi$  goes from 0 to 1, one should fit the data using the following normalized percolation equations,

$$\sigma_m = \sigma_c [(\phi - \phi_c)/(1 - \phi_c)]^t \quad [\phi > \phi_c], \quad (2a)$$

$$\sigma_m = \sigma_i [(\phi_c - \phi)/\phi_c]^{-s} \quad \{\text{or } \epsilon_m = \epsilon_i [(\phi_c - \phi)/\phi_c]^{-s}\} \\ [\phi < \phi_c], \quad (2b)$$

with  $\sigma_c$ ,  $\sigma_i$ ,  $t$ ,  $s$ , and a common  $\phi_c$  as parameters. These equations give  $\sigma_c$  when  $\phi = 1$  and  $\sigma_i$  when  $\phi = 0$ , so that they can, in principle, fit data in the range  $0 \leq \phi \leq 1$ .<sup>12,13</sup>

Until recently it was believed that simulations, based on lattices, and real continuum media both belonged to the same universal class and that  $s$  and  $t$  depended on the dimension of the problem only.<sup>6</sup> The most widely accepted universal values, in three dimensions, are  $s_{un} \approx 0.87$  and  $t_{un} \approx 2.0$ ,<sup>6</sup> but values of  $t$  down to 1.7 are often taken to be acceptable.<sup>1</sup> All computer simulations and many continuum systems supported this belief,<sup>4</sup> but it was also found, in a number of continuum systems, that  $t$  was 3 or even larger.<sup>7,13-16</sup>

Kogut and Straley<sup>17</sup> were the first to show that if the low conductance ( $g$ ) bonds in a percolating resistor network had a distribution  $h(g)$ , characterized by  $h(g) \approx g^{-\alpha}$  with  $0 < \alpha < 1$ , then the conductivity exponent  $t$  would be given by

$$t = t_{un} + \alpha/(1 - \alpha) \quad \text{for } 0 < \alpha < 1, \quad (3a)$$

while for  $\alpha < 0$ ,  $t = t_{un}$ , where  $t_{un}$  is the accepted universal value. For a superconductor-normal resistor network (regime II when  $\sigma_c \rightarrow \infty$ ) with the distribution of normal conductances (now in the  $\sigma_i$  component) with high  $g$ , being characterized by  $h(g) \approx g^{-\beta}$ , the exponent  $s$  would be given by<sup>17</sup>

$$s = s_{un} + (2 - \beta)/(\beta - 1) \quad \text{for } 1 < \beta < 2, \quad (3b)$$

while for  $\beta > 2$ ,  $s = s_{un}$ . Note that this model does not allow either  $s$  or  $t$  to be lower than the accepted universal values of  $s_{un}$  and  $t_{un}$ .

The first model to propose a distribution of the  $g^{-\alpha}$  class, leading to a nonuniversal  $t$  in a continuum system, was the Swiss-cheese model<sup>3,4,18,19</sup> where the narrow conducting necks, joining the larger regions of the conducting material, dominate the resistive behavior. This class of system was realized by Lee *et al.*<sup>16</sup> in a system of glass spheres randomly distributed in indium and gave  $t = 3.1$ . However, the inverted ‘‘Swiss-cheese’’ model was shown not to lead to any change in the transport exponents.

Balberg<sup>20</sup> proposed a model similar to the inverted ‘‘Swiss-cheese’’ model but where the interparticle conduction mechanism is tunneling. This leads to the expression<sup>4,20</sup>

$$t = t_{un} + (a/l)(1 - l/a), \quad (4)$$

where  $a$  is the average closest approach distance between two particles, which could belong to different clusters, and  $l$  is the tunneling distance coefficient. This equation predicts a considerable increase in  $t$  for high  $a/l$ . However, high  $a/l$  values would lead to very resistive media. This model may apply to some carbon black-polymer composites.<sup>20</sup> Further experimental evidence for large  $t$  values, when tunneling is clearly shown to be a dominant conduction mechanism by superconducting measurements, is given in McLachlan *et al.*<sup>13</sup> and Eytan *et al.*<sup>21</sup>

Another model that may allow  $t$  values of somewhat greater than 2 is the links-nodes-blobs (LNB) model of Stanley<sup>22</sup> and Coniglio<sup>23</sup> (see also Ref. 3), which supercedes the oversimplified links-nodes model of de Gennes<sup>24</sup> and Skal and Shklovskii,<sup>25</sup> and provides a realistic picture of the backbone on a lattice and enables the critical exponents to be calculated or estimated. In this picture, a node is any site on the backbone that is connected to the boundaries by at least three independent paths and the internode spacing, above  $\phi_c$ , is the correlation length  $\xi \approx (p - p_c)^{-\nu} [(\phi - \phi_c)^{-\nu}$  in a continuum]. A link consists of lengths of single or cutting bonds (i.e., those which, if cut, will interrupt the current flow) and blobs (which are multiply connected paths on the backbone, where each path carries a fraction of the backbone current). The average resistance of two sites, separated by a percolation correlation length  $\xi$ , or the resistance of the incipient infinite cluster is  $\alpha(p - p_c)^{-\delta}$ , which leads to the expression  $t = \delta + (d - 2)\nu$ .<sup>23,26</sup> If the links are made up of cutting bonds only, the model proposed in Refs. 24 and 25,

$\delta=1$ . According to Refs. 23 and 26, the random resistor model gives  $\delta=1.12$  in 3D, which leads to  $t=1.95$  (1.12 + 0.83). To account for the larger  $t$ , that is found in some continuum system,  $\delta$  would have to be larger than 1.12 (which implies a large fraction of blobs on the backbone). Fisch and Harris<sup>26</sup> give the limit  $\nu < \delta < \nu/\nu_s$ , where  $\nu_s$  is the correlation length exponent for self-avoiding walks. Using their values of  $\nu=0.83$  and  $\nu_s=0.588$ , this gives  $\delta$  an upper limit of 1.49, while  $\nu$  values of 0.83–0.89 have been put forward. Therefore, in its current form, the links, nodes, and blobs model is unable to account for  $t$  values higher than about 2.35 unless, the complexities of the links, nodes, and blobs in a system of real grains (with the possibility of an anisotropic conductivity and/or shape and a range of inter-grain conductances) allows  $\delta$  to be higher than 1.49.

Breakdowns in universality have also been found in two-dimensional anisotropic percolation systems. Model experiments and computer simulations in two dimensions, where both  $s_{\text{un}}$  and  $t_{\text{un}} \approx 1.3$ , give nonuniversal values for  $s$  and  $t$  which, depending on direction, can be either larger or smaller than  $t_{\text{un}}$  (Ref. 4 and the references therein). There appears to be no similar data in three dimensions.

The magnetoresistance of percolating systems has not been extensively studied; there being, to the best of the authors' knowledge, essentially one previous theoretical paper<sup>27</sup> and two experimental studies.<sup>28,29</sup> The Hall effect has been more widely investigated but, as this was not measurable in this system, the reader is referred to the review articles by Bergman and Stroud<sup>3</sup> and Nan.<sup>4</sup> Bergman<sup>27</sup> developed expressions for the low-field Hall effect and magnetoresistance using a scaling approach. For the transverse and longitudinal magnetoresistance two new exponents  $t_{\perp}$  and  $t_{\parallel}$  had to be introduced. Using these it is predicted that, in systems where  $\sigma_c \gg \sigma_i$ ,

$$-\Delta\sigma \propto H^2 \quad \text{and} \quad (\phi - \phi_c)^{t_{\perp} \text{ or } t_{\parallel}} \quad (5a)$$

and

$$\Delta\rho/\rho \propto H^2 \quad \text{and} \quad (\phi - \phi_c)^{t_{\perp} - t \text{ or } t_{\parallel} - t} \quad (5b)$$

Here  $-\Delta\sigma$  is the change in conductivity between zero and a given field, while  $\Delta\rho/\rho$  is the usual  $[\rho(H) - \rho(0)]/\rho(0)$ .

### B. The general effective media equation

Another method of fitting continuum conductivity data ( $\sigma_i/\sigma_c \neq 0$ ), as a function of  $\phi$ , is to use a modification of the general effective media equation proposed by McLachlan<sup>30</sup> and McLachlan, Blaskiewicz, and Newnham.<sup>7</sup> This modification<sup>31</sup> is

$$\frac{(1-\phi)(\sigma_i^{1/s} - \sigma_m^{t/s})}{\sigma_i^{1/s} + A\sigma_m^{1/s}} + \frac{\phi(\sigma_c^{1/t} - \sigma_m^{1/t})}{\sigma_c^{1/t} + A\sigma_m^{1/t}} = 0, \quad (6)$$

where  $A = (1 - \phi_c)/\phi_c$ . This equation reduces to the Bruggeman symmetric equation, when  $t=s=1$ , has the mathematical form of the Bruggeman asymmetric equation, when  $\phi_c=0$  or 1 and  $\sigma_i \rightarrow 0$  or  $\sigma_c \rightarrow \infty$ , and the percolation equations [Eq. (2)] when  $\sigma_i=0$  or  $\sigma_c \rightarrow \infty$  and  $0 < \phi_c < 1$ . It is also a smooth interpolation between the two conductivity equations given in Eqs. (2), when  $\sigma_i/\sigma_c > 0$ .<sup>7,31</sup> When the dc conductivity data in this paper was fitted to both Eq. (2) and

(6), virtually identical values for the parameters were obtained, which is to be expected as  $\sigma_i/\sigma_c \approx 10^{-18}$ . In the results section, the parameters given are usually those obtained from Eq. (2). Note that all three-dimensional data (where  $\sigma_i/\sigma_c$  was usually greater than  $10^{-8}$ ) previously<sup>7,13</sup> fitted to Eq. (6), using  $t=s$ , gave a fit to the data which was as statistically good or nearly as good as that obtained using  $t \neq s$ .

### C. 1/f or flicker noise

Low frequency or 1/f noise has been observed in a wide variety of both homogeneous and percolation systems for many years.<sup>32,33</sup> When a constant "noise free" current is passed through a resistor the observed noise increases; this increase is known as the 1/f or flicker noise. The noise power spectrum in terms of voltage fluctuations is described by Hooge's<sup>34</sup> empirical formula,

$$S_v(f) = \alpha V^2 / (Nf^\gamma), \quad (7)$$

where  $\gamma$  is an exponent close to unity (usually  $\gamma=1.0 \pm 0.1$ ),  $V$  is the dc voltage drop across the sample,  $N$  is the total number of charge carriers in the sample (usually proportional to the volume), and  $\alpha$  is a dimensionless number with a value of the order of  $10^{-5} \rightarrow 10^{-1}$  in small volume metallic samples<sup>32,33</sup> and as high as  $10^3 \rightarrow 10^7$  in granular high- $T_c$  materials.<sup>35</sup>

In this paper after checking that  $S_v$  is proportional to  $V^2$  (or  $I^2 R^2$  as the resistance is Ohmic) and determining  $\gamma$ , the quantity  $S_v/V^2 = \alpha/(Nf^\gamma)$  is examined as a function of  $(\phi - \phi_c)$  or  $R$ , the dc resistance of the sample. Many experimental workers have observed the following power laws in percolation systems:

$$S_v/V^2 = A(\phi - \phi_c)^{-K} \quad (8a)$$

$$= BR^w, \quad (8b)$$

as the percolation threshold is approached from the conducting side. Note that theory predicts that  $w$  should be given by  $w=K/t$ . As the plot of  $S_v/V^2$  against  $R$  should eliminate some of the statistical fluctuations in the  $\sigma_m$  against  $(\phi - \phi_c)$  results, the exponent given in this paper is  $w$ , but  $K$  can be found by multiplying by the appropriate  $t$ . Measurements on percolation systems include those in both two<sup>36–40</sup> and three<sup>41–42</sup> dimensions.

Theoretical calculations give a  $w$  of 0.85 for a three-dimensional random resistor lattice<sup>43,44</sup> and 2.15 for a Swiss-cheese structure.<sup>43</sup> For a three-dimensional Swiss-cheese and inverted Swiss-cheese model, Tremblay, Feng, and Breton<sup>45</sup> calculated  $w$  to be 2.1 and 2.4, respectively. Using a model where the noise is generated in a granular medium by "metal-to-metal" contacts, in the so-called Sharvin regime, Pierre *et al.*<sup>40</sup> obtained a  $w$  of 1.5, for  $\phi > \phi_c$ .

Using scaling arguments Rammal, Tannois, and Tremblay<sup>46</sup> showed that for fractal structure  $S_v(f)/V^2$  is proportional to  $L^{-b}$ , where  $L$  is the linear size of the cubic sample,  $L \ll \xi$ , and  $b$  is a new exponent, with a value of 1.18 for a three-dimensional random resistor network model. While the noise power may scale as  $L^{-b}$  near  $\phi_c$ , it should

scale as  $L^{-3}$  for  $\phi=1$ , i.e., a homogeneous system in three dimensions; the change over should be where  $L \approx \xi$ .<sup>46</sup>

### III. EXPERIMENTAL APPARATUS AND PROCEDURES

All the samples used in these experiments consist of mixtures of graphite powder ( $G$ ) and hexagonal boron nitride (BN) powder together with dry air, as there was always a certain amount of porosity. Graphite and BN are mechanical isomorphs, with almost the same crystal structure (hcp), parameters, and density (2.25 gm/cc). Compressed pellets of the BN, with a porosity of 18% have a resistivity of  $10^{16} \Omega \text{ cm}$  along the direction of compression and  $4.2 \times 10^{14} \Omega \text{ cm}$  at right angles to this direction. Similar compressed graphite pellets have a resistivity along the direction of compression of  $0.12 \Omega \text{ cm}$  and a transverse resistivity of  $2.88 \times 10^{-3} \Omega \text{ cm}$ . For mixed compositions, the appropriate weights of  $G$  and BN were ground together in a planetary mill for an hour. This resulted in a powder in which 80% of the grains lay between 3 and  $24 \mu\text{m}$ .

The first system is the compressed  $G$ -BN series of samples, where disks (diameter 26 mm and thickness about 2.5 mm) were produced in a cylindrical pressure die at 200 Mpa. The porosity of these disks was always very close to 0.18. A comparison of the x-ray spectra of the surfaces of compressed disks and loosely packed powders, showed that during compression the grains oriented, such that 80% of the  $c$  axis lay within one degree of the compression axis. This leads to a large anisotropy in the conductivity. For axial measurements silver paste "capacitor" plates, with two ( $I$  or  $V$ ) loops of thin copper wire embedded in them, were painted on the end faces. For radial measurements bars, with dimensions of about  $24 \times 8 \times 2.5 \text{ mm}$ , were cut from the disks and two or four point leads were attached with silver paste. Note that, because of this geometry, neither capacitive or very high resistivity radial measurements could be made.

The dc conductivity of freshly compacted disk samples near  $\phi_c$  were found to vary fairly rapidly at first and then at an ever decreasing rate. A typical change was 45% in the first ten weeks and then less than 1% in the remainder of a year. All measurements on disk and parallelepiped samples reported here were made on samples aged for at least ten weeks. The origin of this phenomenon is not known and it is planned to investigate it further.

dc resistivity measurements on the low-resistance samples ( $R < 0.1 \text{ M}\Omega$ ) were made using standard procedures and, where necessary, separate  $I$  and  $V$  wires. Resistivity measurements, where  $R > 0.1 \text{ M}\Omega$ , were made using a Keithley 617 operating in the  $V/I$  mode. Capacitance measurements were made using an ESI video bridge. This is an ac vector voltmeter and the separate  $V$  and  $I$  leads were used.

To measure the dependence of  $S_v/V^2$  on the volume of the compressed samples, radial samples (with selected  $\phi$  values) were cut and polished so as to decrease the volume. Typical dimensions are (1)  $18.6 \times 18.6 \times 2.2 \text{ mm}$ , (2)  $16.9 \times 16.9 \times 2.2 \text{ mm}$ , (3)  $14.6 \times 14.6 \times 2.2 \text{ mm}$ , (4)  $12.7 \times 12.7 \times 2.2 \text{ mm}$ , (5)  $11 \times 11 \times 2.2 \text{ mm}$ , (6)  $6.8 \times 6.8 \times 2.2 \text{ mm}$ , (7)  $6.1 \times 6.1 \times 2.2 \text{ mm}$ . In addition two disk samples with a diameter of 50 mm and a thickness 3.8 mm were pressed and  $S_v/V^2$  measured as a function of volume. Typical dimensions here are (1)  $35.1 \times 35.1 \times 3.8 \text{ mm}$ , (2)  $31.4 \times 31.4$

$\times 3.8 \text{ mm}$ , (3)  $25 \times 25 \times 3.8 \text{ mm}$ , (4)  $18 \times 18 \times 3.8 \text{ mm}$  and (5)  $13 \times 13 \times 3.8 \text{ mm}$ . Note that in all these samples it is the area that is being reduced, but as the samples are three dimensional, this should not be important.

The second system consisted of  $G$ -BN 50:50 and 55:45 powders undergoing compression in various piston-cylinder apparatus in which the pressure was applied by a piston, driven by a precision 0.5-mm pitch thread. Reproducible pourings were obtained by pouring the powder into the cylinder through a sieve, which covered the mouth of the cylinder. In one set of measurements the powder was introduced into the slot in a special cylindrical piston, at the bottom to the cylinder. The piston was then raised with a rotating motion, using a screw. In this method the powder underwent no free fall and can be thought of as being "stroked" into position.

The dc powder resistivity measurements were made in cylindrical vessels with internal diameters (ID's) of 42 mm and a length of 90 mm. Preweighed and ground powders of 50%  $G$ -50% BN and 55%  $G$ -45% BN were poured into the cylinders, so as to achieve very low apparent densities. The resistivity measurements were made as the top close fitting nonrotating moving plunger was slowly and incrementally moved down into the cylinder. The volume fraction of the graphite, between the plunger and bottom plate, was accurately known at all times from the weight and density of the graphite and the total volume between the plates, calculated from the accurately known position of the plunger. Near the metal insulator transition (MIT) transition the volume fraction increments were very low, 0.001 (0.1%). For the axial measurements the vessel walls were polyethylene and the metal plunger and bottom of the vessel were the electrodes. For radial measurements the cylindrical vessel walls consist of  $90^\circ$  of brass,  $90^\circ$  of polyethylene,  $90^\circ$  of brass, and again  $90^\circ$  of polyethylene. In this case the plunger and bottom of the vessel are both polyethylene. All the resistivity measurements were made using a Keithley 617 electrometer operating in the  $V/I$  mode.

At the beginning of an experiment the plunger was about 70 mm above the bottom plate and the apparent density about 0.36 gm/cc which corresponds to a packing fraction of about 0.16. The downward motion was limited by the torque that could safely be applied to the 0.5-mm thread. At the lowest point of the motion the plunger was about 40 mm above the bottom plate, the apparent density about 0.63 gm/cc, and the packing fraction about 0.28, which means that there are always air filled cavities in these powders.

The axial ac dielectric (conductivity) measurements were made with the same powders as above, in a cylindrical vessel with an ID of 70 mm and a length of 50 mm. The volume fraction calculations and packing fractions are similar to those described for dc measurements. The dielectric measurements reported here were all made at 100 and 1000 Hz, using an ESI video bridge (vector voltmeter).

As the geometry used for radial resistance measurements was not suitable for capacitance measurements, a different cell geometry had to be used. A slot shaped "cylinder"  $100 \times 100 \times 10 \text{ mm}$  was constructed, where the  $100 \times 100$  faces were the electrodes. The powder was compressed, as above, but using a piston with a face of  $10 \times 100 \text{ mm}$ . The parallelepiped piston-cylinder system was also measured

with no sample present to obtain the capacity of the piston only. After correcting for this, the dielectric constant of the powder was obtained. The measurements were made using the same ESI video bridge.

The samples used for magnetoresistivity measurement were parallelepipeds approximately  $20 \times 2.5 \times 2$  mm in size, the 2-mm edge being in the axial direction. The voltage/current contacts were silver painted onto the  $20 \times 2$  faces, so the current direction (along the 2.5 mm edge) was in a radial direction. The magnetic field, supplied by a conventional 1.5-T iron core magnet, was perpendicular to the 2.5-mm edge, or in the axial direction, which resulted in the transverse magnetoresistance being measured in a radial direction. This is the geometry recommended by Putley<sup>47</sup> to minimize the interference in magnetoresistivity measurements by the Hall effect. The magnetoresistance could only be measured for  $\phi > \phi_c$  and the current and voltage measurements were made using two Digital Multimeters. The magnetic field was measured using a calibrated Hall probe.

An attempt was made to measure the Hall effect in the  $24 \times 8 \times 2.5$  mm radial samples, previously used for resistivity measurements. The current flowed along the 24-mm edge (radial) direction and the field was perpendicular to the  $24 \times 8$  mm plane, i.e., in the axial direction. This was not successful, even though an ac lock-in amplifier technique (to improve the sensitivity and signal-to-noise ratio) was also tried. Attempts to measure the Hall effect at 77 K, were the Hall coefficient of graphite is considerably larger,<sup>48</sup> also failed.

Flicker noise measurements were made on the compacted disks in the axial direction and on the parallelepipeds cut from the discs in the transverse direction. No measurements were made on the powders as the readings were too unstable. Alkaline batteries, wire wound buffer resistors (the total of which was always at least ten times the sample resistance), the sample, and a Stanford Applied Research SR560 low noise preamplifier (running on its internal batteries) were all placed in a grounded shielded steel container. The input impedance of the preamplifier limited the measurements to samples with resistances of less than 100 K $\Omega$ , i.e.,  $\phi > \phi_c$ . The output of the preamplifier went to a HP 3562A Signal Analyzer, which performed fast-fourier transforms to give the noise spectra. The current was varied and calculated, using various buffer resistance-applied voltage combinations in series with the sample, and the measurements were all made at  $20 \pm 1$  °C.

The noise spectrum between 1 and 1000 Hz was taken and averaged over 1000 sweeps by the spectrum analyzer. The flicker noise spectrum was then measured for a number of selected currents, so that the expected current (voltage)  $S_v(f) \propto I^2$  dependencies of spectrum could be verified. These measurements were repeated for a number of axial and radial disk samples, all with approximately the same volume, for different  $\phi$ s ( $\phi > \phi_c$ ). For some selected compositions the noise was measured for various samples, near  $\phi_c$ , with ever decreasing volumes (as previously described).

#### IV. RESULTS

In this section the experimental results and the results of fitting the data to the experimental data will be presented,

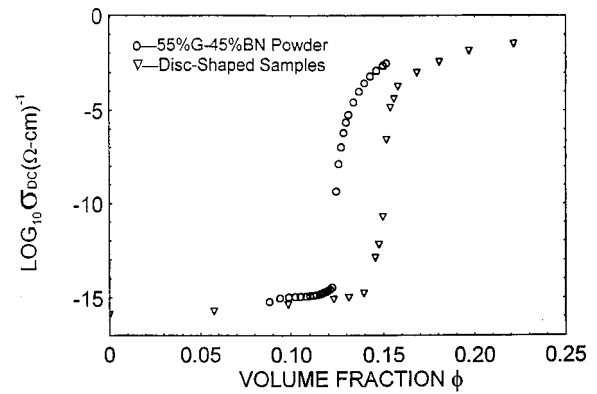


FIG. 1. A plot of the log of the axial dc conductivity  $\sigma_c$  against the volume fraction  $\phi$  for a series of disk-shaped samples and a single run on the 55% graphite-45% boron nitride powder.

with the minimum of discussion. A more detailed discussion will be given in the next section when all the values of  $\phi_c$  and the exponents, together with their experimental uncertainties, have been presented.

In all analysis made in this section the insulating component is a BN-dry air composite. The porosity of all compacted samples, from  $\phi=0$  to 0.82, is close to 0.18. As the BN and graphite grains have the same crystal structure, density and similar size distributions one may consider this series of composites to be such that one starts with a granular BN-air composite and replaces the BN grains by graphite grains as  $\phi$  increases. If this picture is adopted, then one is merely replacing the insulating sites with conducting ones as  $\phi$  increases, and the composite nature of the insulator component is less troublesome. In Fig. 1 plots of the axial conductivity, on a logarithmic scale, for a series of disk samples and a single run on a 55% G-45% BN powder, as a function of  $\phi$  are shown. The large change in the resistivity and the relatively small scatter of the data very near  $\phi_c$ , probably make this the best conductivity data yet observed in a continuum system near  $\phi_c$ . The  $\delta_{dc}$  region, where Eqs. 1(c) apply and given by  $(\sigma_i/\sigma_c)^{1/t+s} = (10^{-16}/10^2)^{1/t+s}$ , is too narrow whether one takes the universal values of  $s$  and  $t$  or the measured ones given below, and no samples lie in this region. The  $\sigma_m$  data shown in Fig. 1 and similar data for another series of disk and powder samples are fitted using equations in Eq. (2), with  $\sigma_c$ ,  $\sigma_i$ ,  $s$ ,  $t$ , and a single value of  $\phi_c$  as parameters. The results of these fits to disk data, shown in Fig. 1, are also plotted in Figs. 2(a) and 2(b). Also shown in Fig. 2(a) is the radial dc conductivity data, for the parallelepiped samples (with  $\phi > \phi_c$ ) cut from the same disk samples shown in Fig. 1, and the best fit to this data. Figure 2(c) shows the data for the capacitive measurements, made at 100 and 1000 Hz, on the insulating side of the above series of disks fitted to the  $\epsilon_m$  equation in Eq. (2). The best fit values of  $s$ ,  $t$ , and  $\phi_c$ , used to plot the theoretical curves in Fig. 2, are given in Table I. Radial conductivity and dielectric measurements on the insulating side of the parallelepiped samples could not be made due to the high resistances and low capacitances, caused by the unfavourable geometric factor. No capacitive measurements could be made on the conducting side of the MIT, due to the high conductivity of the samples and the limitations of the ESI vector voltmeter.

The values of  $\phi_c$ ,  $s$ , and  $t$ , together with the experimen-

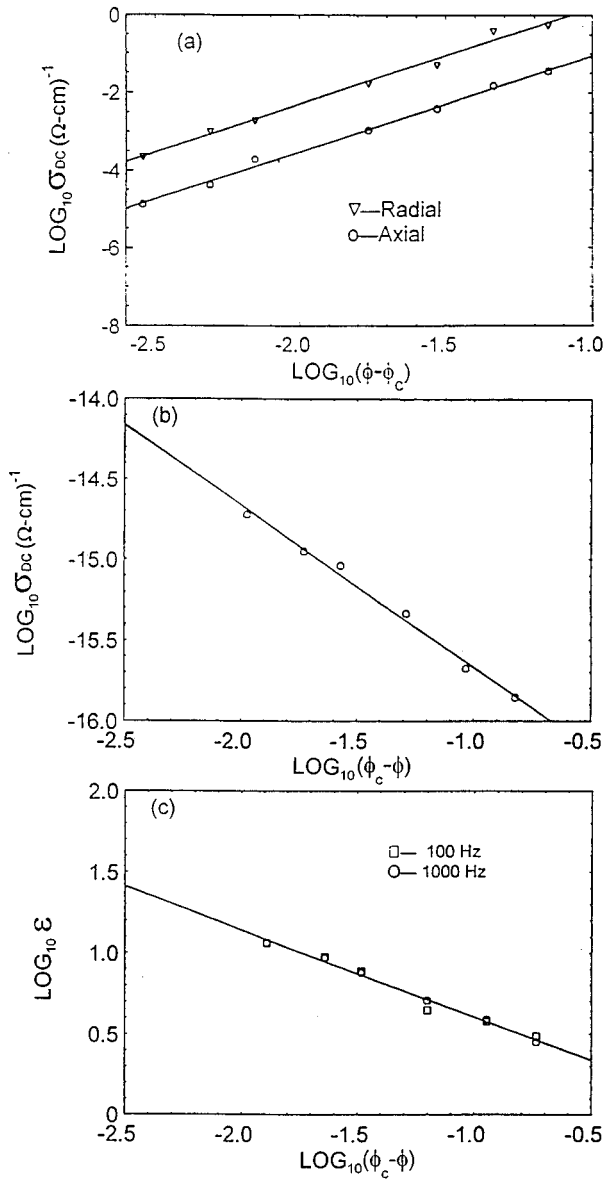


FIG. 2. (a) A plot of the log of the axial and radial dc conductivities ( $\sigma_{dc}$ ) against  $\log_{10}(\phi - \phi_c)$  for compacted disk samples, where  $\phi > \phi_c$ . (b) A plot of the log of the axial dc conductivity ( $\sigma_{dc}$ ) against  $\log_{10}(\phi_c - \phi)$ , where  $\phi < \phi_c$ . (c) A plot of the log of the axial real dielectric constant  $\epsilon$  against  $\log_{10}(\phi_c - \phi)$ , where  $\phi < \phi_c$ .  $\phi_c = 0.150$  in all three cases.

tal uncertainties, obtained for both series of disk samples are summarized in Table I. As previously stated the  $\phi_c$ ,  $\sigma_c$ ,  $\sigma_i$ ,  $s$ , and  $t$  parameters for the axial dc data for disks was obtained from simultaneous fits to Eq. (2). (For brevity the values of  $\sigma_c$  and  $\sigma_i$  are not given in the table, but are mentioned elsewhere in the text.) This method eliminates the problem of getting nearly equally good statistical fits for different combinations of  $\phi_c$  and  $t$ , as emphasized by Lee *et al.*;<sup>16</sup> who suggested that  $\phi_c$  could only be reliably obtained by direct ( $\sigma_m = 0$ ) measurements. However, for real systems ( $\sigma_i/\sigma_c \neq 0$ ), the experimental results depend not only on the system, but also the measuring equipment used (note " $\sigma = 0$ " is very different using a digital multimeter and an electrometer). Therefore, we believe that, where the

TABLE I. This table gives the values of  $\phi_c$ ,  $s$ , and  $t$  obtained from the measurements described in this paper. Values of  $\sigma_c$  and  $\sigma_i$  are mentioned in the text. Axial and radial indicates the direction of the electric field. Direct current measurements are labeled dc while ac measurements are performed at 1000 Hz and sometimes also 100 Hz.

Sample disks	$\phi_c$	$s$	$t$
Axial ac	$0.150 \pm 0.001$	$0.53 \pm 0.07$	$2.58 \pm 0.13$
Axial dc	$0.150 \pm 0.001$	$1.01 \pm 0.05$	$2.63 \pm 0.07$
Radial dc	$0.150 \pm 0.001$		$2.68 \pm 0.13$
"Sieved" powder			
50% G			
Axial ac	$0.114 \pm 0.001$	$0.60 \pm 0.01$	
Axial dc	$0.120 \pm 0.001$	$0.42 \pm 0.01$	$4.85 \pm 0.46$
Radial ac	$0.108 \pm 0.002$	$0.91 \pm 0.02$	
Radial dc	$0.116 \pm 0.003$	$0.26 \pm 0.05$	$6.10 \pm 0.16$
55% G			
Axial ac	$0.124 \pm 0.001$	$0.72 \pm 0.01$	
Axial dc	$0.123 \pm 0.001$	$0.47 \pm 0.01$	$4.80 \pm 0.14$
Radial ac	$0.109 \pm 0.001$	$0.83 \pm 0.06$	
Radial dc	$0.124 \pm 0.001$	$0.46 \pm 0.01$	$6.06 \pm 0.13$
"Poured using a rotating cylinder"			
50% G			
Axial ac	$0.127 \pm 0.001$	$0.53 \pm 0.01$	
Axial dc	$0.123 \pm 0.001$	$0.93 \pm 0.13$	$4.64 \pm 0.04$

data goes over a sufficient range of  $\phi$  on either side of  $\phi_c$ , simultaneous fits to Eq. (2) or a single fit to Eq. (6) are the best methods. The problem of different  $\phi_c - t$  combinations fitting the data nearly equally well is also commented on by McLachlan<sup>12</sup> and Chen and Johnson.<sup>49</sup> The radial parallel-epiped data was fitted to Eq. (1a) only and the best statistical fit parameters are listed. However, the values of  $\phi_c$  and  $t$  tabled for the radial measurements were clearly the best statistical fits, within the error limits. The fact that the  $\phi_c$  (axial) and  $\phi_c$  (radial) values agree with each other to within the experimental accuracy, as is to be expected,<sup>4</sup> increases our confidence in the  $\phi_c$  (radial) and  $t$  values.

Note that the virtually linear and parallel data, for  $\sigma_{dc}$  when  $\phi > \phi_c$ , shown in Fig. 2(a) does not agree with either of the two models proposed by Shklovskii,<sup>50</sup> for the conductivity of anisotropic percolation systems.

The data given in Table I are for disks with a maximum  $\phi$  of 0.24. Conductivity measurements for  $0.82 > \phi > \phi_c$  were also made, using the previously described two embedded wire electrodes or capacitor plates. The data for all the disks from  $\phi = 0$  to  $\phi = 0.82$  is shown in Fig. 3. The theoretical curve shown in Fig. 3 is actually a best fit to Eq. (6) and the parameters are  $\phi_c = 0.150 \pm 0.002$ ,  $\log_{10} \sigma_i = -15.86 \pm 0.04$ ,  $\log_{10} \sigma_c = 1.89 \pm 0.02$ ,  $s = 1.05 \pm 0.18$ , and  $t = 3.03 \pm 0.07$ . These parameters are very close to those obtained using the normalized percolation Eq. (2), for the same data,

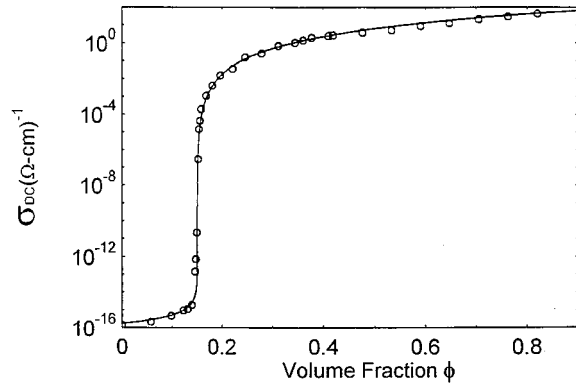


FIG. 3. A plot of the axial dc conductivity, on a log scale, against  $\phi$  for a series of disk-shaped samples over a wider range of  $\phi$  than shown in Fig. 1. The solid line is a best fit to Eq. (6). The parameters are given in the text.

but over a smaller range of  $\phi$ . If Eq. (6) is used to fit the data below  $\phi = 0.24$  only, the results are  $\phi_c = 0.150 \pm 0.002$ ,  $\log_{10} \sigma_i = -15.86 \pm 0.01$ ,  $\log_{10} \sigma_c = 1.50 \pm 0.13$ ,  $s = 1.05 \pm 0.04$ , and  $t = 2.7 \pm 0.24$ , very close to the values given in Table I.

The parameters  $\phi_c$ ,  $\sigma_c$ ,  $\sigma_i$ ,  $s$ , and  $t$  for the axial and radial dc powder data, on both sides of  $\phi_c$ , were also obtained by the simultaneous fit to Eq. (2) method, so there can be very little uncertainty as to their values. The axial and radial capacitive measurements on powders had to be fitted for  $\phi < \phi_c$  only, but the parameters have relatively small error limits. The slightly lower value of  $\phi_c$  for the radial capacitive measurements (compared with the other three) can be attributed to the very different geometry of the "radial" capacitive cell, used in these measurements. The fact that  $\phi_c$  differs by so little, for two rather different geometries (circular and parallelepiped), is actually encouraging. The data and fitted results for the powder experiments are shown in Figs. 4(a), 4(b), and 4(c). The parameters obtained by fitting this data are tabulated in Table I. The ac parameters are those obtained at 1000 Hz. The values measured at 100 Hz were virtually identical.

To check for inconsistencies, each powder experiment was repeated three times and each experiment gave three values for the same parameters  $a_1$ ,  $a_2$ ,  $a_3$  and three statistical standard deviations  $\delta_1$ ,  $\delta_2$ ,  $\delta_3$ . The average value of the parameter was then calculated from the following equation:

$$\bar{a} = [(1/\delta_1^2)a_1 + (1/\delta_2^2)a_2 + (1/\delta_3^2)a_3] / [(1/\delta_1^2) + (1/\delta_2^2) + (1/\delta_3^2)]. \quad (9)$$

The deviation, given with the average parameter in Table I, is the maximum value of  $\delta_1$ ,  $\delta_2$ , or  $\delta_3$ .

The magnetoresistance results are given in Fig. 5 in the form  $\log_{10}[\rho(H) - \rho(0)]/\rho(0)$  against  $\log_{10}(\phi - \phi_c)$ , at  $\mu_0 H = 1.5$  T. The exponent measured is  $0.28 \pm 0.01$ . If  $\log_{10}(-\Delta\sigma(1.5 \text{ T}))$  was plotted against  $\log_{10}(\phi - \phi_c)$  the slope would have been about  $3(t + t_1 = 2.7 + 0.28)$ . The  $(\Delta\rho/\rho)$  slope of 0.28 is in agreement with the value of 0.3 obtained by Rhode and Micklitz<sup>29</sup> for the  $\text{Sn}_x\text{Ar}_{1-x}$  system, but their slope for  $(-\Delta\sigma)$  against  $(\phi - \phi_c)$  is only 1.9, as

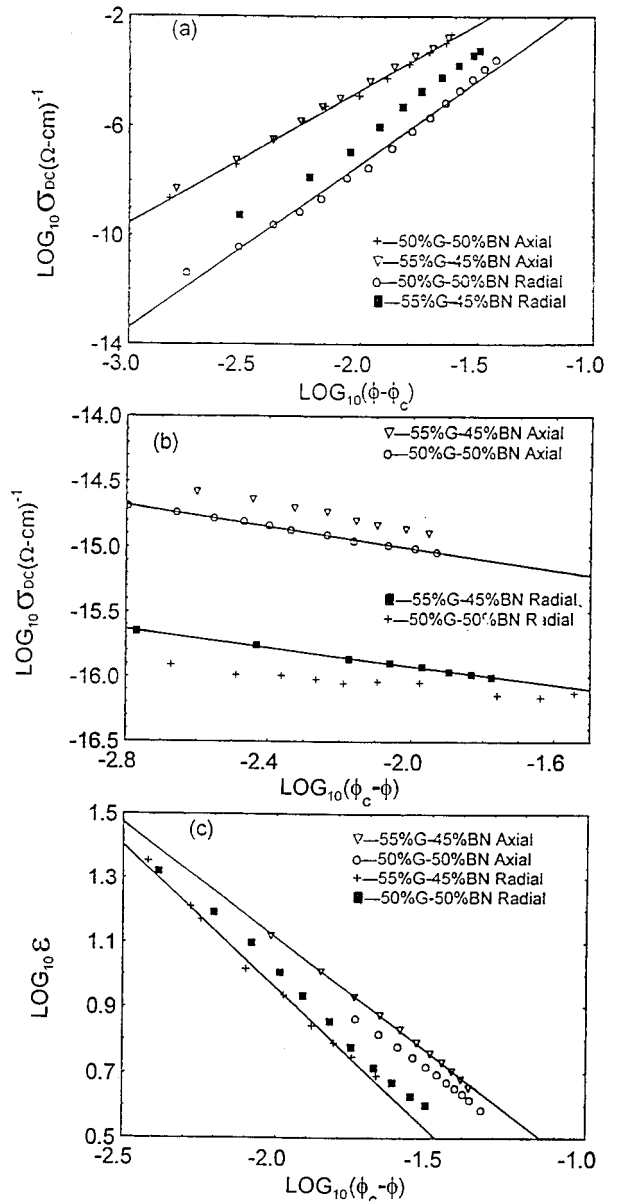


FIG. 4. (a) A plot of the log of the axial and radial dc conductivities ( $\sigma_{dc}$ ) against  $(\phi - \phi_c)$  for 55% graphite-45% boron nitride ( $\phi_c = 0.123$ ) and 50% graphite-50% boron nitride "sieved" powders ( $\phi_c = 0.120$ ) for  $\phi > \phi_c$ , (b) A similar plot to that shown in Fig. 4(a) but the dependent variable is now  $\log_{10}(\phi_c - \phi)$  and  $\phi < \phi_c$ . The  $\phi_c$  value is the same as in Fig. 4(a). (c) A plot of the log of the radial and axial dielectric constants, for the same powders, against  $\log_{10}(\phi_c - \phi)$  for  $\phi < \phi_c$ . Here  $\phi_c$  (radial) = 0.109,  $\phi_c$  (axial) = 0.125, and the frequency is 1000 Hz.

their  $t$  value is 1.6. The question of whether the exponent of about 0.3 for  $(\Delta\rho/\rho)$  against  $(\phi - \phi_c)$  is universal, must await more experiments and further theoretical calculations.

The slopes of the  $-\Delta\sigma$  against  $B_0 = \mu_0 H$  were also examined and best-fit slopes through them were found to be  $1.72 \pm 0.03$ , for  $0.205 \leq \phi \leq 0.24$ , and not 2 as is to be expected [Eq. (5a)]. Rhode and Micklitz<sup>28</sup> give a plot showing a  $H^2$  dependence for  $-\Delta\sigma$  for the  $\text{Bi}_x\text{Kr}_{1-x}$  system, but do not actually show the system to be a percolating one. However, when plotted against  $H^2$  a reasonable straight line can also be drawn through the present results.

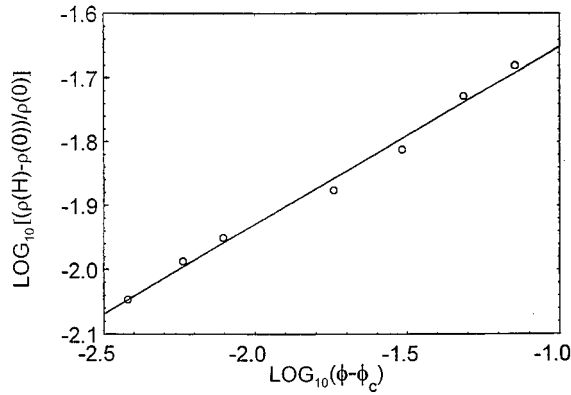


FIG. 5. A plot of the  $\log_{10}$  of  $[\rho(H) - \rho(0)]/\rho(0)$  against  $\log_{10}(\phi - \phi_c)$  [ $\phi_c = 0.150$ ] for radial parallelepiped samples. The slope is  $0.28 \pm 0.01$ .

As previously stated, flicker noise measurements were only made for the axial conducting discs and the parallelepipeds cut from them in the radial direction. Plots of  $\log_{10} S_v$  against  $\log_{10} I$  for several axial and radial samples verify that  $S_v$  is proportional to  $I^2$  (or  $V^2$ ). Plots of  $S_v/V^2$  against the frequency for the axial and radial samples were also made. The observed slopes range between 0.95 and 1.08 with a mean of  $1.04 \pm 0.4$  for the axial samples and the mean is  $1.06 \pm 0.04$  for the radial ones. These slopes are typical for flicker noise.<sup>33,34</sup> Figure 6 shows a plot of  $\log_{10} S_v(10 \text{ Hz})/V^2$  against  $\log_{10} R$  (dc) for both axial disks (the diameter is 26 mm and the thickness is 2.5 mm) and radial parallelepipeds (all close to  $24 \times 8 \times 2.2$  mm), from which values of  $w$  are obtained. When fitted to Eq. (8b), the values for the exponents are  $1.47 \pm 0.08$  in the axial and  $1.72 \pm 0.08$  in the radial direction. The above results are all for samples with nearly the same volume. As one can assume that  $N$  in Eq. (7) is a function of  $\phi$  and total volume, the above measurements were repeated for several radial samples, where the volume was systematically reduced while, it is hoped that,  $\phi$  and  $\phi_c$  remained reasonably constant. These results are given, as a plot of  $S_v(10 \text{ Hz})/V^2$  against the  $\log_{10}$  of the volume in Fig. 7, where some data

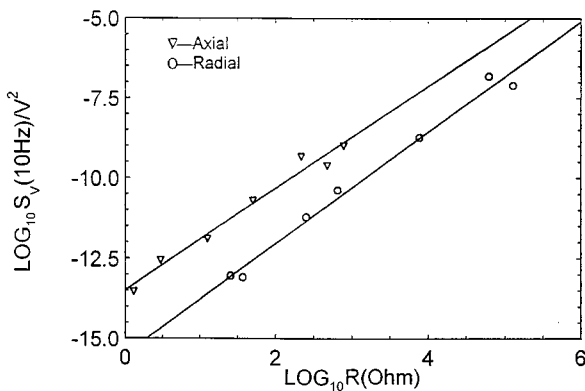


FIG. 6. A plot of  $\log_{10} S_v/V^2$  against  $\log R$  for in both the axial (compacted disks) and radial (parallelepipeds) directions. The exponents are  $1.47 \pm 0.08$  in the axial and  $1.72 \pm 0.08$  in the radial direction.

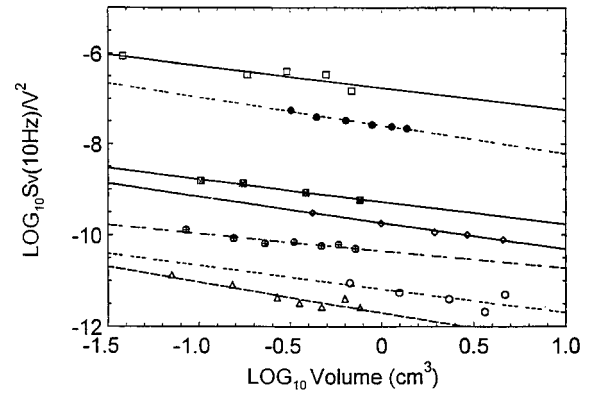


FIG. 7. A plot of  $\log_{10} S_v/V^2$  against the log of the volume of the  $G$ -BN parallelepipeds, for several values of  $\phi$ . The slopes from top to bottom are ( $\square$ )  $-0.49 \pm 0.09$  [ $\phi = 0.156$ ], ( $\bullet$ )  $-0.65 \pm 0.04$  [ $\phi = 0.164$ ], ( $\boxtimes$ )  $-0.50 \pm 0.03$  [ $\phi = 0.164$ ], ( $\diamond$ )  $-0.58 \pm 0.02$  [ $\phi = 0.168$ ], ( $\oplus$ )  $-0.41 \pm 0.07$  [ $\phi = 0.164$ ], ( $\circ$ )  $-0.52 \pm 0.17$  [ $\phi = 0.172$ ], ( $\triangle$ )  $-0.64 \pm 0.09$  [ $\phi = 0.168$ ]. The average of the slopes is  $-0.56$ . The solid lines are plotted with the true values of  $\log_{10}(S_v/V^2)$ , while the broken lines have been shifted in the vertical direction to avoid overlap.

points and the lines through them are shifted up or down for clarity. From Fig. 7 it can be seen that  $S_v/V^2$  is proportional to the volume<sup>-b'</sup>, where the weighted average of  $b'$  is 0.56, and not the volume<sup>-1.0</sup> behavior expected for a homogeneous sample. [Note 0.56 is obtained using a formula similar to Eq. (9)]. The corresponding resistance (very close to proportional to the resistivity) plot against the volume plot has a slope of 1, within the experimental error. None of the previous workers on percolative systems in two<sup>36-40</sup> and three<sup>41,42</sup> dimensions, studied the noise as a function of area or volume.

## V. DISCUSSION

In order to discuss the values of  $\phi_c$ ,  $s$ ,  $t$ , and other exponents given in the previous section and to compare these with the values predicted by lattice models or continuum models, such as the Swiss-cheese model, as well as those observed in other experimental continuum systems, it is necessary to produce reasonable models for the microstructures of the highly compressed disks and lightly compressed powders. This section will therefore start with these models before discussing  $\phi_c$ , the nonuniversal  $s$ , and  $t$ 's and other exponents.

### A. Microstructure of the disks and powders

Stress-strain curves on powder samples show that up to a volume fraction of 0.45 relatively small stresses are compacting the powder and decreasing the size of the cavities. The stresses rise between 0.45 and 0.62 and a sharp rise in the stress at  $\phi = 0.62$  indicates that inelastic strains along the  $a$ - $b$  plane, and possibly even small shards peeling off the grains, are necessary for compression beyond the random close-packed value of the packing (volume fraction). The final structure, with a typical porosity of 18%, is pressure bonded between the  $G$ - $G$ ,  $G$ -BN, and BN-BN grains. The radial electrical resistivity could be primarily determined by the  $G$ - $G$  necks as, the measured resistivities of  $\phi = 0.82$



samples are approximately  $2.9 \times 10^{-3} \Omega \text{ cm}$  along the radial direction, while previously measured single crystal values<sup>48</sup> in the  $a$ - $b$  plane are about  $4.2 \times 10^{-5} \Omega \text{ cm}$ . [Recall that the compressed disks show a strong orientational effect, with the  $c$  axis of the  $G$  and BN grains tending to align along the compression (axial) direction.] If the resistivity is indeed partially determined by the  $G$ - $G$  necks the problem is no longer a pure site one, but is also partially a bond one, as the nearest  $G$  neighbors could be bonded by a range of resistances. As there must be some inelastic flow at the necks (the intergranular contacts), the disk microstructures are analogous to a "binary" Swiss-cheese model, with relatively large area intergranular contacts ( $G$ - $G$ , BN-BN,  $G$ -BN).

Typical size distributions of the starting powders, for both types of experiment, are such that 80% of the grains lies between 3 and 24  $\mu\text{m}$ . An examination of the shape of these ground powders, in a scanning electron microscope, showed the particles to have shapes that can be characterized by a moderate but not an extreme aspect ratio. The starting packing fraction of the  $G$  and BN components was typically 0.16. Taping and shaking the cylinder increased the packing fraction to about 0.20, which is still well below the value of about 0.6 expected for a random close-packed uniform powder. This shows that the starting microstructure for the powder experiments and in the cylindrical mold, before compressing the disks, is one of small air cavities surrounded by the loosely packed  $G$ -BN powder, which contains smaller voids. As the starting volume (packing) fraction of all the powders ( $G$ +BN) used in the powder experiments is about 0.16 and the finishing fraction is about 0.3, the entire powder experiments were done in a region where the grains slip freely over each other and there is no pressure bonding.

### B. The critical volume fraction $\phi_c$

The values of  $\phi_c$ ,  $s$ , and  $t$  obtained from the various experiments are given in Table I. Note that, with one explainable exception, the axial and radial  $\phi_c$ 's are the nearly the same, within the experimental error. This is in accord with<sup>4</sup> and the experimental observations in Ref. 59.

The observed critical volume fraction  $\phi_c$  for the two series of disks of  $0.150 \pm 0.001$  and  $0.153 \pm 0.001$  are within the bounds<sup>10,52</sup> of  $\phi_c = 0.16 \pm 0.2$ , for hard or impermeable spheres of a single size, such that nearest neighbors just touch, placed randomly on all lattices in three dimensions and also random close-packed structures.<sup>10</sup> In the present case the particles are not spherical, and are only approximately the same size. In a series of papers on the concept of the excluded volume, Balberg and his collaborators<sup>53,54</sup> showed that it is normally the excluded volume, given by rotations about the "principal" axis, that determines  $\phi_c$  in random systems. The excluded volume is much larger than the actual volume for extended shapes, such as rods and disks, and the resulting  $\phi_c$  is usually lower than the value of 0.16, expected for the random packing of spheres.<sup>10</sup> For spheres the actual and excluded volumes are the same. In the present case the excluded volume is not too much larger than the actual volume and a value of 0.15 is not unreasonable. In another paper, Balberg *et al.*<sup>53</sup> say in their conclusion "Another increase in the degree of randomness, by allowing objects (grains) of different sizes but of the same shape (into

the composite), does not cause a change in the excluded volume (or  $\phi_c$ )." Therefore we can expect that  $\phi_c$  will not differ much from 0.16, due to the range of particle sizes.

In the powders the values of  $\phi_c$  are typically 0.11 to 0.125. This can be accounted as follows. The microstructure is one of a loosely packed GBN powder, containing voids, surrounding air filled cavities. See illustration in Ref. 51. An analog type of structure was originally considered by Mal'liaris and Turner,<sup>55</sup> but improved upon by Kusy.<sup>56</sup> Kusy argues that, if the conducting particles have a much smaller radius than the insulating (in his case solid) particles, the fine conducting powder will tend to coat the large insulating particles. In the present case the fine powder coating, which forms the walls of the insulating air cavities, contains  $G$ , BN, and small voids between the  $G$  and BN grains, while the larger air filled cavities correspond to the large insulating spheres. When the coating component ( $G$ , BN, air), or in this case the walls of the cavities, are above the percolation limit, the entire three dimensional structure is conducting. As the "large" cavities belong to the insulating fraction this leads to lower values of  $\phi_c$ , as is observed here. Kusy<sup>56</sup> compiled a curve of the ratio of the radius of the insulating grains to the radius of the conducting grains against  $\phi_c$ . The practical minimum  $\phi_c$  for this model is about 0.03. For a  $\phi_c$  of 0.1, according to Kusy's curve, the ratio of the radii of the mean insulating particle (or in this case, the mean air filled cavity) to the mean conducting particle size is about 7. It is therefore apparent that a large number of insulating particles or cavities with a size of about 7 times the typical size of the conducting grains can lead to  $\phi_c$ 's well below 0.10. Cavities of this size (30–100  $\mu\text{m}$ ) would be hard to get rid of by pressure.

### C. The critical exponents $s$ and $t$

From the microstructures just discussed, the structure of the compressed disk composites is that of a "binary" ( $G$ +BN) anisotropic inverted Swiss-cheese model, with voids. According to Feng, Halprih, and Sen<sup>19</sup> the (single component plus voids) inverted Swiss-cheese structure does not have the wide range of conductance necessary to give rise to a non-universal  $t$  and should be characterized by a universal  $t$ . We believe the same to be true in the present case. Another mechanism for an increased  $t$  is an inverted Swiss-cheese model with a barrier tunneling between the grains,<sup>20</sup> but as there are no oxide or polymer coatings between the tightly compressed and bonded graphite grains, tunneling cannot occur along the current carrying backbones of this  $G$ -BN system. Another mechanism, the increase in  $t$  due to the anisotropy of the conductivity, has to date only been extensively investigated (experiments and computer simulations) in two dimensions (Ref. 4 and the references therein). Here it is found that while the  $t$  in one direction increases with anisotropy, in the other direction it decreases. This could be, but is probably not, a feature of two dimensional systems only. As, in the present case,  $t$  is approximately equal in both directions in the compressed disk series of  $G$ -BN samples, this "mechanism" can probably be ruled out.

Another consideration is the influence of the porosity (microvoids) of the disks and the cavities and voids in the powder samples. Still another is that, although the variation of

the conductivity with  $\phi$  is consistent with a site percolation problem (with a nonuniversal  $t$ ), the idea of a simultaneous bond percolation problem must be considered, to account for the variation of intergranular contact resistances. As these two considerations are probably only relevant in the powder experiments, they will only be discussed as a possible explanation for the very high  $t$  values obtained for the powder samples. As previously discussed the powders, which form or coat the insulating cavities, must be visualized as a conductor-insulator mixture of the two components and voids surrounding air filled cavities. As a powder "coating" approaches and passes through the percolation threshold, the powder "coating" density increases (smaller voids) and the air filled cavities shrink (some may even vanish). For powders, as can be seen from Figs. 4(a) and 4(b), the axial conductivities are always higher than the radial ones at and on both sides of  $\phi_c$ , which is the opposite of what is observed for the compressed disks. This could be due to the intergrain pressure being higher in the axial (compression and gravity) direction than the radial one. Although the axial and radial dc conductivities give the same  $\phi_c$ , the different exponents show that the axial and radial directions are not equivalent in a percolative sense. There could, in both the axial and radial directions, be a contribution to the enhancement of  $t$  from the large range of intergranular conductances,<sup>17</sup> that is likely to occur in a poured and lightly compressed powder. This could be one of the reasons why the radial direction, probably with smaller intergranular contact pressures and hence a larger range of intergranular conductivities, has a larger  $t$ . As this proposed wide range of intergranular contact resistances are not created by scalloped intergranular necks, as proposed in Refs. 18, 19, the expressions in these papers cannot be used to estimate  $t$ .

What has been discussed above is a site-range of bond (intergranular) resistivities model. But, if some of the neighboring graphite grains (sites) just fail to make contact, being held apart by "wedge edges" of neighboring BN grains, this would give the system some aspects of a site-bond percolation problem. However this, while changing  $\phi_c$ , is not supposed to give a nonuniversal  $t$ .<sup>57</sup> Also it is not very likely that many intergraphite grain distances will be in the correct range for vacuum tunneling and these will invariably be short circuited by actual contacts between grains. Hence no  $t$  enhancement can be expected from the tunneling mechanism for the powder experiments. Therefore, it would appear that the enhancement of  $t$ , in the powder experiments, could be due to a large range of intergranular conductances and/or possibly the cavity containing structure.

The presence of cavities have not yet been incorporated into any lattice simulations and model experimental systems and probably occur in many other continuum composites. Further evidence for the cavity or large insulating sphere structure giving high- $t$  values, is given by the experiments on thick-film glass-RuO<sub>2</sub> resistors,<sup>14</sup> which also show a very high- $t$  values (3–5). The microstructure here is one where conducting percolating filaments of RuO<sub>2</sub> or Bi<sub>2</sub>Ru<sub>2</sub>O<sub>7</sub> (obtained from a powder whose radius is much smaller than that of the glass beads) encapsulate the glass beads. The  $\phi_c$ 's for these resistors is very low ( $\phi_c \leq 0.021$ ), which is in accord with the results of Kusy,<sup>56</sup> but this structure and the resultant  $\phi_c$ 's can also be understood in terms of the grain consolida-

tion model.<sup>58</sup> Carmona *et al.*<sup>15</sup> also remark on the analogies between their carbon fiber-polymer geometry (with  $t$ 's up to 3.5) and that of the thick-film resistors. These support our contention that the cavities and microstructure of percolating powders surrounding them, are a possible cause of the high- $t$  values.

Deprez and McLachlan<sup>59</sup> made powder compression experiments, which were analogous to the present ones, except that the measurements were made using four different (resistivity and grain shape) pure graphite powders and hence only for  $\phi > \phi_c$ . They obtained  $t(\phi_c)$  values, for the axial and transverse directions, respectively, of  $1.94 \pm 0.05(0.295 \pm 0.004)$  and  $2.8 \pm 0.3(0.27 \pm 0.02)$  for natural flaky graphite powder,  $2.7 \pm 0.05(0.315 \pm 0.01)$  and  $2.7 \pm .01(0.33 \pm 0.01)$  for technical graphite powder,  $1.52 \pm 0.03(0.27 \pm 0.01)$  and  $2.1 \pm 0.2(0.25 \pm 0.02)$  for synthetic graphite powder and  $1.5 \pm 0.04(0.38 \pm 0.04)$  and  $2.4 \pm 0.05(0.37 \pm 0.015)$  for electrographite dust powder. These results show that particles with different shapes and anisotropic conductivities can lead to different and often anisotropic  $t$  values, in powder compression and probably other experiments. Note that it is always  $t$  (axial) that is lower than  $t$  (transverse) when the anisotropic ratio of the  $t$ 's is greater than one. This differs from the two-dimensional data quoted in Nan<sup>4</sup> but, as for this graphite it is the conductivity tensor rather than the geometric shape that is anisotropic, this may not be of any significance. These and the present results indicate that the  $\phi_c$  and  $t$  values obtained for powder compression experiments depend very much on the powders used. This must be due to the way that the different powders pack, which includes the number and nature of the cavities and the range of intergranular conductances, which naturally occur in a particular powder (single or multicomponent). A reexamination of the results of Deprez and McLachlan<sup>59</sup> shows that for the NFG and TGP powders the transverse conductivities are always greater than the axial ones. In the SGP powder there is a crossover and in the EGD powder the axial conductivity is always greater than transverse, as is observed for the  $G$ -BN powders. As the NFG powder has the most flaky  $G$  grains, the EGD powder the most "spherical"  $G$  grains<sup>59</sup> and the present powder also has fairly spherical grains, this shows that the shapes of the grains are probably playing an important role. These pure graphite systems are probably closer to a pure site one, because close neighbors cannot be held apart by BN "wedges." Therefore, as nearly the same  $\phi_c$  is observed for different pouring methods in the current experiments,  $\phi_c$  would appear to depend more on the geometries and compositions of the powders, than the way that it is poured (note the range of  $\phi_c$ 's observed by Deprez and McLachlan<sup>59</sup>). It should also be noted that Chen and Johnson<sup>49</sup> obtained a lower  $\phi_c(0.075)$  and a higher  $t(3.1)$  for filamentary nickel than for nodular nickel ( $\phi_c=0.265$  and  $t=2.2$ ), both in polypropylene. It would therefore appear that these "geometric effects" are not confirmed to anisotropic conductors like graphite.

The expected value for the exponent  $s$  from computer simulations is 0.87–0.89,<sup>6</sup> while from Table I it can be seen that a large range of  $s(0.26–1.06)$  has been obtained in the present experiments. Unfortunately, there is no clear pattern to the results. For the compressed disks the  $s$  obtained from the real part of the dielectric constant is clearly smaller than that obtained from the dc conductivity, while for the powders

poured through a sieve undergoing compression the reverse is the case. In the powders, poured using a rotating cylinder, the  $s$  values are more similar to these for compressed disks. This could be due to the  $c$  axis of the grains in this powder tending to more strongly align along the axial direction, as it does in the compressed disks. The powder results also show that the powders poured by different methods give  $\phi_c$ 's that are closer to each other than the corresponding  $s$  values. This shows that the exponent  $s$  is probably more sensitive to the details of the microstructures of the powders or disks, long-range correlations in the system, than is  $\phi_c$ . However, this does not appear to be the case for the  $t$  exponent. Differences in the  $s$  exponent between the dc and ac results could be because the ratio of the dielectric constants is about three, while that between the conductivity of BN and dry air is not known and may not be very constant from day to day. (Pumping the air out of the powder is not feasible as the flowing air changes its structure.) One important feature of percolation theory is that  $s$  and  $t$  should not depend on the relative conductivities or dielectric constants of the components, but there is now some evidence to the contrary.<sup>60</sup> As previously argued for the  $t$  exponent, the predictions for a larger than universal  $s$  (Refs. 17, 19) do not apply for the compressed disks, where the dc axial  $s$  value is greater than one, as they have an anisotropic inverted "Swiss-cheese" structure.

The authors can find no other values of  $s$  obtained by ultrahigh resistivity measurements. Conductivity measurements for  $\phi < \phi_c$  have also been made on granular<sup>13,31</sup> and random<sup>31,61</sup> Al-Ge films where, in both cases,  $\sigma_i/\sigma_c$  is only about  $10^{-7}$ .

An examination of previous values obtained for  $s$  from experimental dielectric measurements gives  $s = 0.73 \pm 0.07$  ( $\phi_c = 0.20 - 0.22$ ) for silver particles in a KCl matrix,<sup>62</sup>  $s = 0.68 \pm 0.05$  ( $\phi_c = 0.29$ ) for amorphous carbon in teflon,<sup>63</sup> and  $s = 0.55 \pm 0.10$  ( $\phi_c = 0.075$ ) and  $s = 0.62 \pm 0.10$  ( $\phi_c = 0.265$ ) for filamentary and nodular nickel, respectively.<sup>49</sup> These values tend, except for our anomalous 0.93 value, to be a little higher than those obtained in the present experiments. However, a pattern is emerging that the values of  $s$  for three dimensional continuum systems, obtained by capacitive experiments, tend to be lower than the ("universal") values obtained from computer simulations.

#### D. Conductivity anisotropy, magnetoresistivity, and noise

Shklovskii's models<sup>50</sup> for the anisotropy of the conductivity do not apply to these systems and there appears to be no other theories for this phenomenon. As there are only two magnetoresistivity results a comparison of the exponents from experimental results is perhaps premature. However, the fact that the same value for  $t_{\perp} - t$  is obtained for two systems, with very different  $t$  values, is intriguing.

The results for the noise measurements are given in terms of the exponent  $w$ , as this is how experimental results are most often presented, because it is then not necessary to determine  $\phi_c$  and  $t$  and there is a reduction on the experimental error compared with a  $S_v/V^2$  against  $\phi - \phi_c$  plot. The unfortunate result of this practice is that one cannot always correlate  $w$  with  $t$  and  $\phi$  in the literature. In all of the two-dimensional experiments on percolation systems<sup>36-40</sup>

only  $w$  is given and the values range from 1.18 to 6.2. This is probably due to the wide variety of methods used to vary the resistance of the film (ion-milling, sand blasting, temperature, and during film deposition). However, these results do show that  $w$  is not a universal constant. The three-dimensional results of Chen and Chou<sup>41</sup> on carbon-wax mixtures are the very similar to the present ones. Their results for  $\phi_c$  and  $t$  are 0.108 and 2.3, though a refit of their data<sup>12</sup> gives 0.109 and 4.0, but their  $w$  result of  $1.7 \pm 0.2$  is independent of the  $\phi_c$  and  $t$  values obtained by fitting. This  $w$  value agrees very well with the present radial value of  $1.72 \pm 0.08$  and is in fair agreement with the axial value of  $1.47 \pm 0.08$ . The equivalence of the two systems depends largely on whether or not there is intergranular barrier tunneling in carbon-wax mixtures, i.e., does the wax wet the carbon grains and is there an intergranular wax tunneling barrier. A comparison of the  $w$  values indicates that, either there is no barrier tunneling in the carbon-wax system, or that barrier tunneling does not contribute to the noise, which is thought to be unlikely. As the carbon was stirred into a very viscous wax,<sup>41</sup> just below the melting point, it is highly likely it did not wet the carbon. The results of Rudman, Calabreze, and Garland<sup>42</sup> on Ag-Pt powder in PTFE powder give a  $w$  of 3.0 near  $\phi_c$  and a  $w$  of 1.0 further away from  $\phi_c$ .

As has previously been argued we believe the compressed disks to have an anisotropic inverted Swiss-cheese structure, but the values of 1.47 and 1.72 are both lower than the  $w$  of 2.15 calculated by Rammal *et al.*<sup>44</sup> or the  $w$  value of 2.4 calculated by Tremblay, Feng, and Breton.<sup>45</sup> However, the present values are close to the intergranular "metal-to-metal" contact model of Pierre *et al.*,<sup>40</sup> which gives  $w = 1.5$ , in both two and three dimensions. This is also the value observed in a two-dimensional monolayer or near monolayer of clean copper spheres in a polymer.<sup>40</sup> The system in Ref. 40 is a two-dimensional inverted Swiss-cheese structure with small contact areas. However, there is no reason that this current contact model should not apply to a three-dimensional inverted Swiss-cheese system, with relatively large contact areas.

The observed volume <sup>$\approx -0.56$</sup>  contrasts with the volume <sup>$-1$</sup>  or  $N^{-1}$  behavior [Eq. (7)] expected for a homogeneous sample. This should correspond to a length <sup>$-1.68$</sup>  dependence, if the composite is homogeneous or  $L \gg \xi$ . The 1.68 is to be contrasted with the value of 1.18 (length <sup>$-1.18$</sup> ) obtained by Rammal, Tannois and Tremblay<sup>46</sup> on a random resistor model, near the percolation threshold, where the resistor clusters are fractals. We do not believe that the compressed disks closely resemble the random resistor model, but do believe the graphite clusters to be fractal sufficiently close to  $\phi_c$ . Rammal, Tannois, and Tremblay<sup>46</sup> state, but do not prove in their paper, that the factor 1.18 should increase in a continuum medium, such as the  $G$ -BN systems. Girand *et al.*<sup>64</sup> obtained length <sup>$-1.0$</sup>  in a two dimensional hierarchical deterministic fractal lattice.

For the sample closest to  $\phi_c$ ,  $\phi - \phi_c \approx 0.001$  and as the mean grain size is  $\approx 10 \mu\text{m}$ ,  $\xi = a/(\phi - \phi_c)^{0.85} \approx 3 \text{ mm}$ , which is close to the thickness of the samples. However, as the results are consistent and extend out to  $\phi - \phi_c \approx 0.1$  and  $\xi = 0.07 \text{ mm}$ , it can be assumed that the samples are all homogeneous and three dimensional in the sense that  $L > \xi$ .

## VI. CONCLUSIONS

As with most experimental papers on percolative systems, this paper has concentrated on measuring an electrical response of the system to an external simulation, and then fitting the results to the appropriate percolation equation. Where successful this results in a critical volume fraction or percolation threshold ( $\phi_c$ ) and an exponent, which can be different above and below  $\phi_c$ , being evaluated for each response measured. It is now widely accepted that there is no universal value for  $\phi_c$ , as this depends on the details of the microstructure<sup>7,54,58</sup> and not only on the dimension of the system. Experimental results, especially for the widely measured dc conductivity and ac dielectric constants, already quoted in this paper, show that percolation equations [Eq. (2)] fit the experimental results for systems with a wide range of values of  $\phi_c$ , both above and below the “true random” value of 0.16 (Refs. 52, 63, 65) being obtained. Because the experimental results for  $\phi_c$  obtained in this paper, from various measurements on the same system, are very consistent with each other and adequate explanations for their values have already been given, this will not be further discussed. Instead, this conclusion section will concentrate on the “universal or otherwise” values obtained for the exponents.

In the words of Lee *et al.*,<sup>16</sup> one can only expect a universal exponent if the local microstructure is isotropic and contains only short-range correlations. It can also be expected that a topological exponent such as  $\xi$ , the correlation length exponent, will be less sensitive to the distinction between lattice or continuum systems,<sup>66</sup> than exponents such as  $s$  and  $t$ , especially if the conducting component is an anisotropic conductor.

Furthermore, Rammal *et al.*<sup>44</sup> and Archangels, Redner, and Coniglio<sup>67</sup> have shown that the distribution of currents in fractal resistor networks can be discussed in terms that relate directly to a hierarchical LNB model and multifractals and that these distributions are characterized by a hierarchy of exponents. Unfortunately, at this stage, the exponents  $s$  and  $t$  cannot be calculated using this approach.

Therefore, taking all the factors that may affect  $s$  and  $t$  into account, it should come as no surprise that very complex systems, such as those studied in this paper, do not exhibit “universal” exponents. Rather the surprise should be that the electrical responses, as a function of conductor concentration in very complex systems, such as those measured here, can be described by simple scaling expressions, such as

the percolation power laws. The microstructure in both of the present systems include a nonisotropic conductor and a microvoid (disks) or void and cavity (powders) structure (which may give medium- or long-range correlations). In the lightly compressed powder samples, a large range of intergranular (cluster) resistances may enhance  $t$ .

That a microstructure containing cavities does not automatically lead to a higher  $t$  can be seen from the experimental results of Deprez, McLachlan, and Sigalas<sup>51</sup> who obtained a value for  $t$  of 1.7 for sintered Ni-air. As the values of  $t$  (1.5–2.8), obtained from compressing pure graphite powders<sup>59</sup> are considerably lower than for similar experiments with  $G$  (0.50 and 0.55)-BN powders ( $t=4.6$ –6.1), the existence of percolation channels in the powder “coatings” of the voids or insulating cavities may be a crucial factor. The only other very high  $t$  values are for RuO<sub>2</sub> resistors<sup>14</sup> ( $t=2.85$ –5.01) and Bi<sub>2</sub>Ru<sub>2</sub>O<sub>7</sub> resistors ( $t=5.46$ –6.87), and may also be due to percolating channels of conducting oxide around the large glass grains. This type of structure is being further investigated.

Most of the values of  $s$  obtained here and all those in other dielectric experiments are lower than the values, presumably universal, obtained from lattice simulations. The reasons for this are not clear, but the distributions of the real and displacement currents in a continuum are far more complex than in a lattice model where, in the simplest models, each bond carries either a real or a displacement current. More investigations, both experimental and theoretical, are needed if a satisfactory explanation for these results is to be found.

For the other parameters our main conclusion is that more experiments, where a large range of electrical responses are measured on the same system, are essential if correlations between the exponents  $s$ ,  $t$ , ( $\lambda$ ),  $t_{\perp}$  and  $t_{\parallel}$ ,  $w$ , and  $b'$  are to be found in real continuum systems.

## ACKNOWLEDGMENTS

The authors would like to thank Dr. A. Albers for his technical assistance and advice and Professor L. Schoening for the interpretation of the x-ray results, obtained by J. Salemi. We are also grateful to M. Van Nierop and Professor M. H. Moys for doing the particle sizing, Professor D. Chandler for the work on the universal testing machine, Professor H. Hanrahan for the loan of the HP 3562A signal analyzer, and the staff of our Electron Microscope Unit.

<sup>1</sup>S. Kirkpatrick, *Rev. Mod. Phys.* **45**, 574 (1973).

<sup>2</sup>R. Landauer, in *Electrical Transport and Optical Properties of Inhomogeneous Media*, edited by J. C. Garland and D. B. Tanner, AIP Conf. Proc. No. 40 (AIP, New York, 1978), p. 2.

<sup>3</sup>D. J. Bergman and D. Stroud, *Solid State Physics, Advances in Research and Applications*, edited by H. Ehrenreich and D. Turnbull (Academic, San Diego, 1992), Vol. 46, p. 147.

<sup>4</sup>Ce-Wen Nan, *Prog. Mater. Sci.* **37**, 1 (1993).

<sup>5</sup>G. Deutscher, R. Zallen, and J. Adler, *Ann. Isr. Phys. Soc.* **5**, (1983).

<sup>6</sup>D. S. Stauffer and A. Aharony, *Introduction to Percolation Theory*, 2nd ed. (Taylor and Francis, London, 1994).

<sup>7</sup>D. S. McLachlan, M. Blaskiewicz, and R. F. Newnham, *J. Am. Ceram. Soc.* **73**, 2187 (1990).

<sup>8</sup>A. L. Efros and B. I. Shklovskii, *Phys. Status Solidi B* **76**, 475 (1976).

<sup>9</sup>D. J. Bergman and Y. Imry, *Phys. Rev. Lett.* **39**, 1222 (1977).

<sup>10</sup>R. Zallen, *The Physics of Amorphous Solids* (Wiley, New York, 1983), Chap. 4.

<sup>11</sup>J. P. Straley, *J. Phys. C* **9**, 783 (1976).

<sup>12</sup>D. S. McLachlan, *Solid State Commun.* **60**, 821 (1986).

<sup>13</sup>D. S. McLachlan, R. Rosenbaum, A. Albers, G. Eytan, N. Grammatika, G. Hurwits, J. Pickup, and E. Zaken, *J. Phys. Condens. Matter* **5**, 4829 (1993).

- <sup>14</sup>G. E. Pike, in *Electrical Transport and Optical Properties of Inhomogeneous Media* (Ref. 2), p. 366.
- <sup>15</sup>F. Carmona, P. Prudhon, and F. Barreau, *Solid State Commun.* **51**, 255 (1984).
- <sup>16</sup>S. Lee, Y. Song, T. Noh, and J. R. Gaines, *Phys. Rev. B* **34**, 6719 (1986).
- <sup>17</sup>P. M. Kogut and J. P. Straley, *J. Phys. C* **12**, 2151 (1979).
- <sup>18</sup>B. I. Halprin, S. Feng, and P. N. Sen, *Phys. Rev. Lett.* **54**, 2391 (1985).
- <sup>19</sup>S. Feng, B. I. Halprin, and P. N. Sen, *Phys. Rev. B* **35**, 197 (1987).
- <sup>20</sup>I. Balberg, *Phys. Rev. Lett.* **59**, 1305 (1987).
- <sup>21</sup>G. Eytan, R. Rosenbaum, D. S. McLachlan, and A. Albers, *Phys. Rev. B* **48**, 6362 (1993).
- <sup>22</sup>H. E. Stanley, *J. Phys. A* **10**, L211 (1977).
- <sup>23</sup>A. Coniglio, *J. Phys. A* **15**, 3829 (1982).
- <sup>24</sup>P. G. de Gennes, *J. Phys. (France) Lett.* **37**, L1 (1976).
- <sup>25</sup>A. Skal and B. I. Shklovskii, *Fiz. Tekh. Poluprovodn.* **8**, 1568 (1974) [*Sov. Phys. Semicond.* **8**, 1024 (1975)].
- <sup>26</sup>R. Fisch and A. B. Harris, *Phys. Rev. B* **18**, 416 (1978).
- <sup>27</sup>D. J. Bergman, *Philos. Mag. B* **56**, 983 (1987).
- <sup>28</sup>M. Rhode and H. Micklitz, *Phys. Rev. B* **36**, 7572 (1987).
- <sup>29</sup>M. Rhode and H. Micklitz, *Physica A* **157**, 120 (1989).
- <sup>30</sup>D. S. McLachlan, *J. Phys. C* **20**, 865 (1987).
- <sup>31</sup>D. S. McLachlan, *Electrically Based Microstructural Characterization*, edited by R. A. Gerhardt, S. R. Taylor, and E. J. Garboczi, MRS Symposia Proceeding No. 411 (Materials Research Society, Pittsburgh, to be published), p. 309.
- <sup>32</sup>P. Dutta and P. H. Horn, *Rev. Mod. Phys.* **53**, 497 (1981).
- <sup>33</sup>M. B. Weissman, *Rev. Mod. Phys.* **60**, 537 (1988).
- <sup>34</sup>F. N. Hooge, *Phys. Lett.* **29A**, 139 (1969).
- <sup>35</sup>Yi Song, A. Misra, Yue Cao, A. Querubin, Xiao-Deng Chen, P. P. Crooker, and J. R. Gaines, *Physica C* **172**, 1 (1990).
- <sup>36</sup>R. H. Koch, R. B. Laibowitz, E. I. Alessandrini, and J. M. Viggiano, *Phys. Rev. B* **32**, 6932 (1985).
- <sup>37</sup>G. A. Garfunkel and M. B. Weissman, *Phys. Rev. Lett.* **55**, 296 (1985).
- <sup>38</sup>J. V. Mantese and W. W. Webb, *Phys. Rev. Lett.* **55**, 2212 (1985).
- <sup>39</sup>M. Octavia, G. Gutierrez, and J. Aponte, *Phys. Rev. B* **36**, 2461 (1987).
- <sup>40</sup>C. Pierre, R. Deltour, J. van Bentum, J. A. A. J. Perenboom, and R. Rammal, *Phys. Rev. B* **42**, 3380 (1990); **42**, 3386 (1990).
- <sup>41</sup>C. C. Chen and Y. C. Chou, *Phys. Rev. Lett.* **54**, 2529 (1985).
- <sup>42</sup>D. A. Rudman, J. J. Calabreze, and J. C. Garland, *Phys. Rev. B* **33**, 1456 (1986).
- <sup>43</sup>R. Rammal, *Phys. Rev. Lett.* **55**, 1428 (1985).
- <sup>44</sup>R. Rammal, C. Tannons, P. Breton, and A.-M. S. Tremblay, *Phys. Rev. Lett.* **54**, 1718 (1985).
- <sup>45</sup>A.-M. S. Tremblay, S. Feng, and P. Breton, *Phys. Rev. B* **33**, 2077 (1986).
- <sup>46</sup>R. Rammal, C. Tannois, and A.-M. S. Tremblay, *Phys. Rev. A* **31**, 2662 (1985).
- <sup>47</sup>E. H. Putley, *The Hall Effect and Related Phenomena* (Butterworths, London, 1960).
- <sup>48</sup>W. N. Reynolds, *Physical Properties of Graphite* (Elsevier, New York, 1968).
- <sup>49</sup>I. G. Chen and W. B. Johnson, *J. Mater. Sci.* **26**, 1565 (1991).
- <sup>50</sup>B. I. Shklovskii, *Phys. Status Solidi B* **85**, K111 (1978).
- <sup>51</sup>N. Depreez, D. S. McLachlan, and I. Sigalas, *Solid State Commun.* **66**, 869 (1988).
- <sup>52</sup>H. Scher and R. Zallen, *J. Chem. Phys.* **53**, 3759 (1970).
- <sup>53</sup>I. Balberg, C. H. Anderson, S. Alexander, and N. Wagner, *Phys. Rev. B* **30**, 3933 (1984).
- <sup>54</sup>I. Balberg, *Philos. Mag. B* **56**, 991 (1987).
- <sup>55</sup>A. Malliaris and D. T. Turner, *J. Appl. Phys.* **42**, 614 (1971).
- <sup>56</sup>R. P. Kusy, *J. Appl. Phys.* **48**, 5301 (1977).
- <sup>57</sup>B. Jouchier, C. Allain, B. Gauthier-Manuel, and E. Guyon, *Ann. Isr. Phys. Soc.* **5**, 167 (1983).
- <sup>58</sup>D. S. McLachlan, *J. Appl. Phys.* **70**, 3681 (1991).
- <sup>59</sup>N. Deprez and D. S. McLachlan, *J. Phys. D* **21**, 101 (1988).
- <sup>60</sup>J. J. Lin, *Phys. Rev. B* **44**, 789 (1991).
- <sup>61</sup>J. Shoshany, V. Goldner, R. Rosenbaum, M. Witcomb, D. S. McLachlan, A. Palevski, M. Karpovski, A. Gladkikh, and Y. Lereah, *J. Phys. Condens. Matter* **8**, 1729 (1996).
- <sup>62</sup>D. M. Grannan, J. C. Garland, and D. B. Tanner, *Phys. Rev. Lett.* **46**, 375 (1981).
- <sup>63</sup>Yi Song, T. W. Noh, S.-I. Lee, and J. R. Gaines, *Phys. Rev. B* **33**, 904 (1986).
- <sup>64</sup>G. Girand, J. P. Clerc, B. Orsal, and J. M. Laugier, *Europhys. Lett.* **318**, 935 (1987).
- <sup>65</sup>J. P. Fitzpatrick, R. B. Malt, and F. Spaepen, *Phys. Lett.* **47A**, 207 (1974).
- <sup>66</sup>M. A. Dubson, Y. C. Hui, M. B. Weissman, and J. C. Garland, *Phys. Rev. B* **39**, 6807 (1989).
- <sup>67</sup>L. de Arcangelis, S. Redner, and A. Coniglio, *Phys. Rev. B* **31**, 4725 (1985); **34**, 4656 (1986).